ANALYSIS OF THERMOMECHANICAL BEHAVIORS OF A FUEL ELEMENT USING THREE DIMENSIONAL ISOPARAMETRIC FINITE ELEMENTS*

S. D. YU and S. XU

Department of Mechanical Engineering, Ryerson Polytechnic University
350 Victoria Street, Toronto, Ontario, Canada M5B 2K3

ABSTRACT

In this paper, three dimensional heat transfer in a nuclear fuel element consisting of UO_2 pellets and Zircaloy sheath is investigated using the finite element method. Nine node isoparametric elements are used in conjunction with the Fourier series for the modeling of three dimensional behavior of heat conduction in a system of axisymmetric solids. The nonlinear simultaneous equations of heat conduction are solved using the iterative approach. A computer program - FUEL3D is developed and used to obtain numerical simulation results for two heat transfer problems in a CANDU fuel element.

INTRODUCTION

A three dimensional analysis of thermomechanical behaviors in a CANDU fuel element may be necessary if non-uniform heat transfer across the radial gap between the sheath and pellets, axial heat transfer via end caps, non-uniform heat generation in the axial direction and thermal anisotropy of UO_2 are to be considered. Modeling of thermomechanical behavior of a nuclear fuel element is a challenging task because of various complicating factors such as nonlinear thermomechanical properties of materials, coupling between heat transfer and mechanical deformations through solid-solid contacts, complex geometry of pellets, etc. To properly model the thermomechanical behaviors of a nuclear fuel, the finite element method is used in this paper.

Hsu [1] studied axisymmetric heat transfer problems in a two dimensional solid using the finite element method. Tayal [2] investigated the two dimensional steady state nonlinear heat transfer problems in a nuclear fuel element utilizing the FEAT code developed by him using three node triangular finite elements. The transient heat transfer features were added to the FEAT code by Tayal et al. [3] in the assessment of fuel temperature under an accidental scenario.

Because of the axisymmetry of the fuel element geometry, all thermal field variables are periodic functions of θ in the cylindrical coordinates. They can be expanded into Fourier series in the circumferential direction. Variations in the other two directions are taken into

* Presented at the 6th International Conference on CANDU Fuel, Niagara Falls, Ontario, Canada. September 26-30, 1999

consideration using two dimensional finite elements. In this paper, the nine node isoparametric elements were chosen as the two dimensional finite elements for modeling of the three dimensional thermomechanical behaviors in the nuclear fuel. Use of this type of elements has several advantages - improved accuracy with geometric (angular) element distortion, quadratic polynomial for temperature gradient within each element, and continuous temperature gradient along element boundaries. These features are important in determining the degree of accuracy and the rate of convergence for calculations of temperatures in the nuclear fuel.

In this paper, all thermal and mechanical properties are assumed to vary with the spatial variables in a manner identical to the field temperature. This practice further enhances the accuracy of computed temperatures and the convergence rate.

Numerical results for temperatures in the fuel element calculated using FUEL3D, a computer program developed by the authors, are compared with the analytical solution for a one dimensional heat transfer problem. The agreement is excellent for the one dimensional case. Test cases for three dimensional heat transfer in a nuclear fuel element are being developed. In this paper, only the isotherms and heat flux vector on different surfaces for a three dimensional heat transfer problem in the nuclear fuel were presented.

MATHEMATICAL PROCEDURE

In this section, the equation of heat conduction in a heterogeneous and anisotropic solid is presented in a cylindrical coordinate system. The nonlinear equations of heat conduction for nodal temperatures in a nuclear fuel element consisting of two distinct solids - pellets and sheath are derived from the Galerkin method.

Governing Differential Equation

According to Hsu [1], the steady state heat conduction in a solid is governed by the following equation

$$-\nabla \cdot \vec{q} + H = 0 \tag{1}$$

where H is the heat generation rate per unit volume; ∇ is the gradient operator; $\vec{q}$ is the heat flux vector defined in terms of temperature gradient ∇T and thermal conductivity matrix $[k]$ as

$$\vec{q} = -[k] \cdot \nabla T \tag{2}$$

In dealing with the heat transfer problems in a nuclear fuel element, it is preferable to work with the cylindrical coordinates r, θ and z. In this case, the conductivity matrix and gradient operator are written as

$$[k]=\begin{bmatrix} k_{rr} & k_{r\theta} & k_{rz} \\ k_{\theta r} & k_{\theta\theta} & k_{\theta z} \\ k_{zr} & k_{z\theta} & k_{zz} \end{bmatrix}, \quad \nabla=\begin{Bmatrix} \dfrac{\partial}{\partial r} \\ \dfrac{\partial}{r\partial\theta} \\ \dfrac{\partial}{\partial z} \end{Bmatrix} \tag{3}$$

where $[k]$ is the thermal conductivity matrix for a thermally anisotropic solid. The governing differential equation of heat conduction in a solid may be written in the following matrix form

$$\begin{Bmatrix} \dfrac{\partial}{\partial r} \\ \dfrac{\partial}{r\partial\theta} \\ \dfrac{\partial}{\partial z} \end{Bmatrix}^T \begin{bmatrix} k_{rr} & k_{r\theta} & k_{rz} \\ k_{\theta r} & k_{\theta\theta} & k_{\theta z} \\ k_{zr} & k_{z\theta} & k_{zz} \end{bmatrix} \begin{Bmatrix} \dfrac{\partial T}{\partial r} \\ \dfrac{\partial T}{r\partial\theta} \\ \dfrac{\partial T}{\partial z} \end{Bmatrix} + H = 0 \tag{4}$$

Because the thermal conductivity components of a solid vary with temperature, the above heat conduction equation is nonlinear. It is difficult to obtain an analytical solution to the nonlinear heat conduction equation for solids of arbitrary shapes, arbitrary boundary conditions, and variable heat generation rate. In this paper, the finite element method is used to obtain an approximate numerical solution to Equation (4).

Finite Element Formulation

To obtain a solution using the finite element method, the entire domain that a solid of interest occupies, V, is divided into N_e sub-domains (finite elements) such that $V = V_1 \cup V_2 \cup \ldots \cup V_{N_e}$. Within each sub-domain, V_e, $e = 1,2,\ldots N_e$, an approximate solution $T_e(\theta, r, z)$ is sought in terms of shape function matrix $[N(\theta, r, z)]$ and nodal temperatures $\{T\}_e$ as follows

$$T_e(\theta, r, z) = [N(\theta, r, z)]\{T\}_e \tag{5}$$

Within each finite element, the approximate solution $T_e(\theta, r, z)$ satisfies the following weak form of governing equation

$$\sum_{e=1}^{N_e}\left[\iiint_{V_e} \phi_e \nabla\cdot[k]\cdot\nabla T_e dV + \iiint_{V_e} \phi_e H dV\right] = 0 \tag{6}$$

where ϕ_e is an arbitrary but admissible temperature distribution in V_e. In a finite element application, ϕ_e is assumed to take on the following form

$$\phi_e(\theta,r,z)=\{\phi\}_e^T[N(\theta,r,z)]^T \tag{7}$$

where $\{\phi\}^e$ is an arbitrary and admissible nodal temperatures.

Upon substitution of Equations (5) and (7) into Equation (6) and utilization of Gauss's divergence theorem, the weak form of equation is written as

$$\sum_{e=1}^{N_e}\left[\{\phi\}_e^T[K]_e\{T\}_e\right]+\sum_{e=1}^{N_e}\{\phi\}_e^T\oiint_{S_e}[N]^T\vec{q}\cdot d\vec{S}=\sum_{e=1}^{N_e}\{\phi\}_e^T\{Q\}_e \tag{8}$$

Because of the arbitrariness of $\{\phi\}_e$, we have

$$\sum_{e=1}^{N_e}[K]_e\{T\}_e+[K_b]\{T\}=\sum_{e=1}^{N_e}\{Q\}_e+\{Q_b\} \tag{9}$$

where $\{T\}$ is the global nodal temperature vector; $[K_b]$ and $\{Q_b\}$ are the boundary conductance matrix and boundary load vector, which are discussed in the assembly of element equations; the element conductance matrix and thermal load vector, $[K]_e$ and $\{Q\}_e$, are determined by

$$[K]_e=[L]_e^T\iint_{A_e}\left\{\int_0^{2\pi}\begin{bmatrix}\dfrac{\partial[N]}{\partial r}\\ \dfrac{\partial[N]}{r\partial\theta}\\ \dfrac{\partial[N]}{\partial z}\end{bmatrix}^T[k]\begin{bmatrix}\dfrac{\partial[N]}{\partial r}\\ \dfrac{\partial[N]}{r\partial\theta}\\ \dfrac{\partial[N]}{\partial z}\end{bmatrix}d\theta\right\}rdrdz[L]_e$$

$$\{Q\}_e=[L]_e^T\iint_{A_e}\left\{\int_0^{2\pi}[N]^T H d\theta\right\}rdrdz$$

where $[L]_e$ is a sparse transformation matrix that rearranges the elements in the natural nodal temperature vector for the purpose of direct assembly of element conduction equations.

For an axisymmetric solid, the entire volume may be represented by a finite number of annuli. A typical annulus or an axisymmetric finite element is shown in Figure 1. Because of the axisymmetry of the solid geometry, the field temperature along with all other thermal variables is a periodic function of θ. It can therefore be represented by

$$T_e = \begin{bmatrix} 1 & \cos\theta & \sin\theta & \cdots & \cos n\theta & \sin n\theta \end{bmatrix} \begin{Bmatrix} T_0(r,z) \\ T_1(r,z) \\ T_2(r,z) \\ \vdots \\ T_{2n}(r,z) \\ T_{2n+1}(r,z) \end{Bmatrix}_e = \begin{bmatrix} N_\theta \end{bmatrix} \begin{Bmatrix} T_0(r,z) \\ T_1(r,z) \\ T_2(r,z) \\ \vdots \\ T_{2n}(r,z) \\ T_{2n+1}(r,z) \end{Bmatrix}_e \tag{10}$$

where n is the order of harmonics retained in an analysis; the harmonic compositions T_k are functions of r and z only. Each harmonic composition T_k may be determined using the shape function matrix and its nodal values in the r and z plane. For a nine node isoparametric element, this relation may be written as

$$T_k(r,z) = \begin{bmatrix} N_1(\xi,\eta) & N_2(\xi,\eta) & \cdots & N_9(\xi,\eta) \end{bmatrix} \begin{Bmatrix} T_{k,1} \\ T_{k,2} \\ \vdots \\ T_{k,9} \end{Bmatrix} = \begin{bmatrix} N_{\xi,\eta} \end{bmatrix} \{T_k\}_e \tag{11}$$

where $N_{\eta\xi}$ is the shape function matrix for a nine node isoparametric element; ξ, η are nondimensional coordinates that define the position of a material point within element e; $\{T_k\}_e$ is the nodal temperature vector associated with the k-th harmonic composition in the Fourier series representation. The transformation between the coordinates r, z and ξ, η is defined by the same shape function, or

$$r = \begin{bmatrix} N_{\xi,\eta} \end{bmatrix} \begin{Bmatrix} r_1 \\ r_2 \\ \vdots \\ r_9 \end{Bmatrix}_e = \begin{bmatrix} N_{\xi,\eta} \end{bmatrix} \{r\}_e, \quad z = \begin{bmatrix} N_{\xi,\eta} \end{bmatrix} \{z\}_e \tag{12}$$

where $\{r\}_e$ and $\{z\}_e$ are the radial and axial coordinates of the nine nodes for element e.

The element conductance matrix and element thermal load vector for a geometrically axisymmetric solid may be determined using the following shape function matrix

$$[N] = [N_\theta] \underbrace{\begin{bmatrix} [N_{\xi,\eta}] & & & \\ & [N_{\xi,\eta}] & & \\ & & \ddots & \\ & & & [N_{\xi,\eta}] \end{bmatrix}}_{2n+1 \text{ submatrices}} \tag{13}$$

In carrying out the integrals, the numerical integration in the circumferential direction is calculated first using the Fast Fourier Transform. Integrals in the (r, z) plane is then calculated numerically using the 4×4 point Gaussian quadrature. In the preparation of the element conductance matrix, each thermal conductivity component is assumed to vary according to the shape function matrix. Nodal values of the conductivity matrix are calculated from nodal temperatures using MATPRO correlations recommended by INSC [4]. In the case of axisymmetric solid, matrix $[L]_e$ defines the following transformation

$$\left\{ \{T_0\}_e \quad \{T_1\}_e \quad \cdots \quad \{T_n\}_e \right\}^T \xrightarrow{[L]_e} \left\{ \underbrace{\{T_0 \quad T_1 \quad \cdots \quad T_n\}}_{\text{node 1}} \quad \cdots \quad \underbrace{\{T_0 \quad T_1 \quad \cdots \quad T_n\}}_{\text{node 9}} \right\}^T \tag{14}$$

Global Equations of Heat Transfer and Boundary Conditions

Once the conductance matrices and load vectors for all finite elements are completed, they can be assembled to form the following global equation of conduction

$$[K]\{T\} = \{Q\} \tag{15}$$

Before solving the simultaneous equations for temperatures, the global conductance and thermal load vector must be modified to satisfy the imposed boundary conditions. Two types of boundary conditions are of interest in this paper - convective heat transfer boundary conditions at the sheath outer surface and combined heat transfer boundary conditions at the interface between the pellet outer surface and sheath inner surface. For the convective boundary conditions, the global heat conductance matrix and global thermal load vector may be modified by adding the following boundary matrix for each surface element consisting of three node

$$[K_b]_1 = \sum_{e=1}^{N_{e1}} [L_1]_e^T \iint_{S_{e,1}} \underbrace{\begin{bmatrix} N_\xi & & & \\ & N_\xi & & \\ & & \ddots & \\ & & & N_\xi \end{bmatrix}}_{2n+1 \text{ submatrices}}^T [N_\theta]^T h_c [N_\theta] \underbrace{\begin{bmatrix} N_\xi & & & \\ & N_\xi & & \\ & & \ddots & \\ & & & N_\xi \end{bmatrix}}_{2n+1 \text{ submatrices}} r d\theta dz [L_1]_e \tag{16}$$

$$\{Q_{b,1}\} = \sum_{e=1}^{N_{e1}} [L_1]_e^T \iint_{S_{e,1}} \underbrace{\begin{bmatrix} N_\xi & & & \\ & N_\xi & & \\ & & \ddots & \\ & & & N_\xi \end{bmatrix}}_{2n+1 \text{ submatrices}}^T [N_\theta]^T h_c T_\infty r d\theta dz \tag{17}$$

where h_c is the convective heat transfer coefficient; $[L_1]_e$ is a sparse matrix that transforms the local nodal temperatures to their global positions for a three node surface element; N_{e1} is the number of surface elements having convective boundary conditions; T_∞ is the coolant temperature; N_ξ is the shape function matrix for a three node line element.

For the combined heat transfer boundary conditions between the pellet and the sheath, an effective heat transfer coefficient, h_{ps}, is introduced. The heat transfer boundary conditions at the pellet outer surface and sheath inner surface may be written as

$$\bar{q}_p = h_{ps}\left(T_p - T_s\right),\ \bar{q}_s = h_{ps}\left(T_s - T_p\right) \tag{18}$$

Substituting the above equation into the surface integral in Equation (8), one obtains the following global boundary matrix, which need be added to the global heat conductance matrix to satisfy the combined heat transfer boundary conditions

$$[K_b]_2 = \sum_{e=1}^{N_{e2}} [L_2]_e^T \begin{bmatrix} K_{b,2}^e & -K_{b,2}^e \\ -K_{b,2}^e & K_{b,2}^e \end{bmatrix}^T [L_2]_e \tag{19}$$

where $[L_2]_e$ is a sparse matrix that transforms the local nodal temperatures to their global positions for a three node gap element; N_{e2} is the number of gap elements having combined boundary conditions; matrix $K_{b,2}^e$ is determined by

$$\left[K_{b,2}^e\right] = \iint_{S_{e,2}} \underbrace{\begin{bmatrix} N_\xi & & & \\ & N_\xi & & \\ & & \ddots & \\ & & & N_\xi \end{bmatrix}}_{2n+1 \text{ submatrices}}^T [N_\theta]^T h_{ps} [N_\theta] \underbrace{\begin{bmatrix} N_\xi & & & \\ & N_\xi & & \\ & & \ddots & \\ & & & N_\xi \end{bmatrix}}_{2n+1 \text{ submatrices}} r d\theta dz \tag{20}$$

It is noted that in carrying out the surface integrals, the two heat transfer coefficients h_{ps} and h_c are allowed to vary in the circumferential and axial directions.

NUMERICAL RESULTS

Convergence Tests

Convergence tests were conducted for two heat transfer problems described in Table 1 where geometric parameters are taken from Reference [5]. Case 1 concerns a one dimensional heat conduction problem in two axisymmetric solids with convective and combined heat transfer boundary conditions. Case 2 involves a three dimensional heat transfer problem. For the two cases, impact of mesh size and number of iterations on computed temperature was investigated. It can be seen that a mesh size of 2 mm, which translates into 32 elements and 170 nodes, and two iterations are necessary to achieve an accuracy of ±1 °K. Use of very fine mesh increases the computation time significantly while providing very little improvement in accuracy. These findings are illustrated in Figure 2. Numerical simulations performed using a SUN station indicate that an appropriate finite element mesh for the temperature obtained with acceptable accuracy and acceptable computing time has an average element size of 1 to 2 mm.

One Dimensional Heat Transfer

In the case of one dimensional heat transfer, the heat conduction equation in the pellet and sheath may be reduced to

$$\frac{1}{r}\frac{d}{dr}\left(rk_p\frac{dT_p}{dr}\right)+H=0,\quad \frac{1}{r}\frac{d}{dr}\left(rk_s\frac{dT_s}{dr}\right)=0 \tag{21}$$

The convective and combined heat transfer boundary conditions may be written as

$$\begin{gathered}T_p(r)\Big|_{r=0}\neq\infty,\ -k_p\frac{dT_p}{dr}\Big|_{r=a}=h_{sp}(T_p-T_s)\Big|_{r=a}\\ -k_s\frac{dT_s}{dr}\Big|_{r=a}=-k_p\frac{dT_p}{dr}\Big|_{r=a},\quad -k_s\frac{dT_s}{dr}\Big|_{r=b}=h_c(T_s-T_\infty)\Big|_{r=b}\end{gathered} \tag{22}$$

Exact solutions for temperatures in the pellet and the sheath after incorporating the above boundary conditions may be obtained for constant thermal conductivities k_p and k_s, and uniform heat generation rate. They are written as

$$\begin{gathered}T_p(r)=\frac{H}{4k_p}(a^2-r^2)+T_\infty+\frac{Ha}{2}\left(\frac{1}{h_{ps}}+\frac{a}{bh_c}+\frac{a}{k_s}\ln\frac{b}{a}\right)\qquad(0\le r\le a)\\ T_s(r)=\frac{Ha^2}{2k_s}\ln\frac{b}{r}+T_\infty+\frac{Ha^2}{2bh_c}\qquad(a\le r\le b)\end{gathered} \tag{23}$$

Results for a one dimensional heat transfer problem described in Table 1 were calculated using FUEL3D and the analytical solutions. Figure 3 shows that the results from FUEL3D are identical to those analytical solutions for temperature in the pellet midplane.

Three Dimensional Heat Transfer

Analysis of a three dimensional heat transfer problem described in Table 1 was conducted using the finite element mesh shown in Figure 4. The driving factors for the three dimensional heat transfer are circumferential variation of effective heat transfer coefficient across the radial gap between the pellet and the sheath, chamfer and dish. The heat flux vector field and isotherms in plane $\theta = 0^{\circ}$ are shown in Figures 5 and 6. These two figures clearly show the axial heat transfer because of the chamfer and dish. The circumferential variation in h_{ps} causes heat transfer in the circumferential direction. As a result, the isotherms in the pellet midplane ($r - \theta$) are different from perfect circles as shown in Figure 7.

CONCLUSIONS

This paper presents a three dimension finite element analysis of heat conduction in a nuclear fuel element. Numerical results obtained for a one dimensional heat transfer problem are in agreement with the analytical solution. Convergence rate for the nonlinear temperature calculations is excellent. Only three iterations are required to achieve an accuracy of ±1 °K. The same type of element is now being implemented in FUEL3D for modeling of thermally induced elastic-creep deformations of a nuclear fuel element.

ACKNOWLEDGMENTS

The authors would like to thank Mr. M. Tayal and Mr. J. H. K. Lau of Atomic Energy of Canada Ltd. (AECL) for their valuable suggestions and support, and the National Science and Engineering Research Council (NSERC) of Canada for its funding through a research grant.

REFERENCES

1. T.-R. Hsu 1986 *The Finite Element Methods in Thermomechanics*, Allen & Unwin, Boston, MA.
2. M. Tayal 1989 "The Finite Element Code FEAT to Calculate Temperatures in Solids of Arbitrary Shapes," *Nuclear Engineering and Design* **114**, 99-114.
3. M. Tayal, S. D. Yu, C. Manu, R. Aboud, D. Bowslaugh, L. Flatt 1997 "Modelling Transient Two-Dimensional Non-Linear Temperatures In Nuclear Fuel Using The Feat Code", *Proceedings of the 5th International Conference on CANDU Fuel*, Toronto, Ontario, Canada, 352-363.
4. International Nuclear Safety Center (INSC), Material Property Database, available electronically at //www.insc.anl.gov/matprop/.
5. J. J. Duderstadt and L. J. Hamilton 1976 Nuclear Reactor Analysis, John Wiley and Sons, Inc., Toronto, Canada.

TABLE 1 DESCRIPTIONS OF TWO HEAT TRANSFER PROBLEMS

Parameters	Case 1	Case 2
Pellet outer radius (mm)	6.00	6.00
Sheath inner radius (mm)	6.00	6.08
Sheath thickness (mm)	0.40	0.40
Pellet full length (mm)	19.00	19.00
Chamfer height (mm)	0.00	0.50
Chamfer width (mm)	0.00	1.00
Dish depth (mm)	0.00	0.20
Dish radius (mm)	0.00	3.50
UO_2 thermal conductivity W/mK	4.00	INSC Database
Zircaloy thermal conductivity W/mK	16.00	INSC Database
Heat transfer coefficient between pellet and sheath kW/m^2K	1.50	1.50(1+0.1cosθ)
Heat transfer coefficient between sheath and coolant kW/m^2K	50.00	50.00
Coolant temperature K	578.00	578.00
Uniform eat generation rate MW/m^3	442.10	442.10
Number of harmonics n	1	1
Boundary conditions on other surfaces	$q_n = 0$	$q_n = 0$

TABLE 2 CONVERGENCE TEST - MAXIMUM TEMPERATURE VS. MESH SIZE

Cases Studied	Average Mesh Size			
	3.0 mm	2.0 mm	1.0 mm	0.75 mm
Case 1	2519.5 K	2519.5 K	2519.5 K	2519.5 K
Case 2	2281.5 K	2261.6 K	2261.0	2261.2

TABLE 3 CONVERGENCE TEST - MAXIMUM TEMPERATURE VS. ITERATIONS

Cases Studied	Max iterations to achieve ±1 °K accuracy (mesh size of 2.0 mm)		
	1	2	3
Case 1	2519.5 K	2519.5 K	-
Case 2	2249.4 K	2261.6 K	2261.6 K

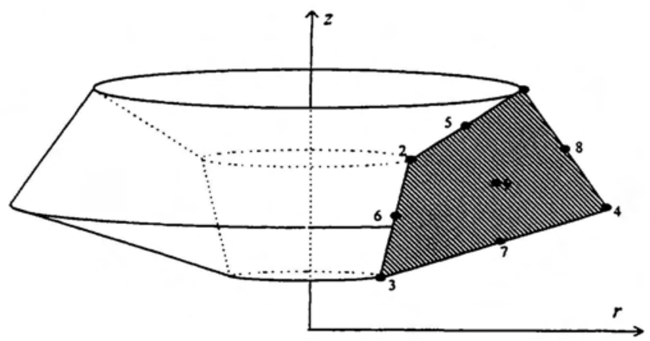

FIGURE 1 A TYPICAL NINE NODE FINITE ELEMENT IN AN AXISYMMETRIC SOLID

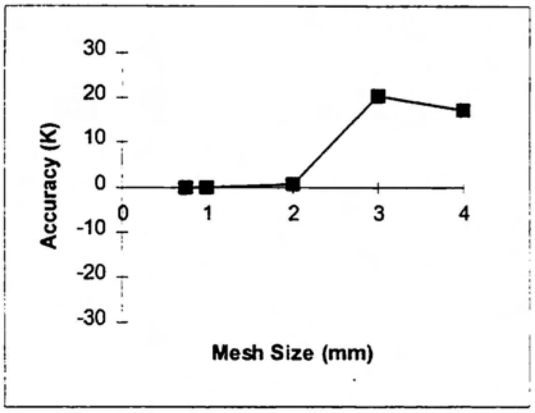

(a)

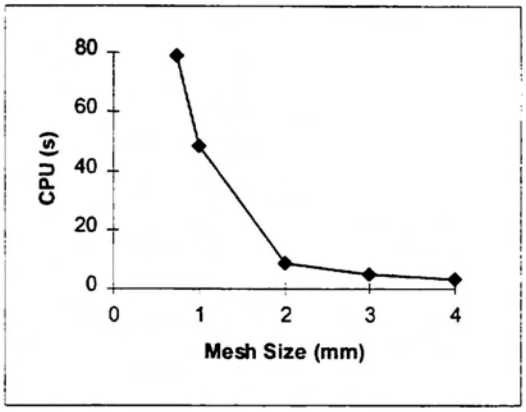

(b)

FIGURE 2 (a) ACCURACY VS. MESH SIZE; (b) COMPUTING TIME VS. MESH SIZE

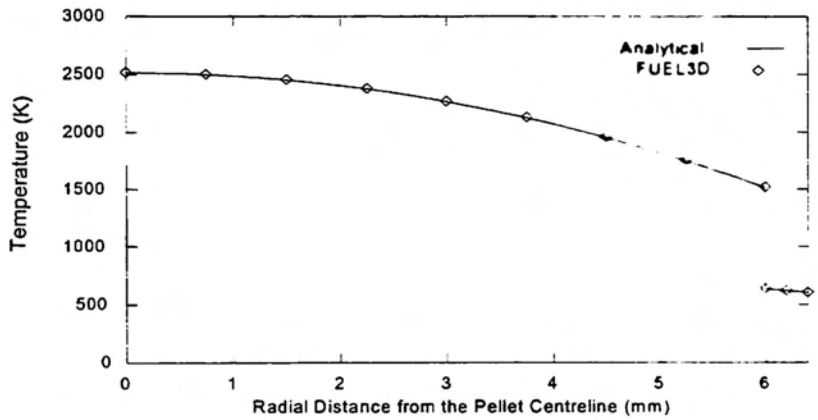

FIGURE 3 TEMPERATURE PROFILE IN FUEL ELEMENT (CASE 1)

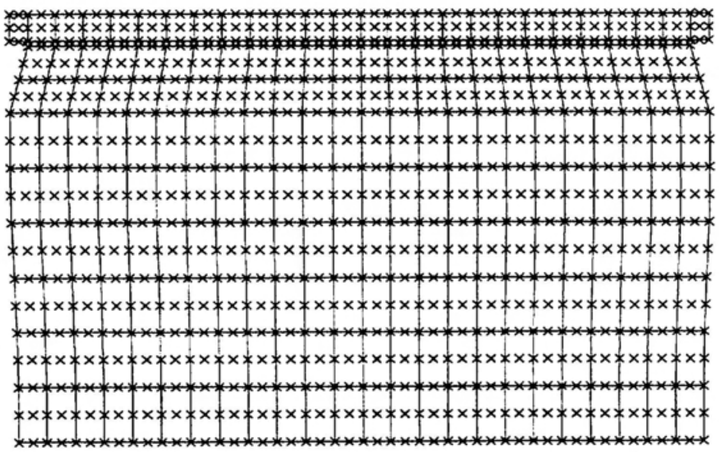

FIGURE 4 A FINITE ELEMENT MESH USED IN CASE 2

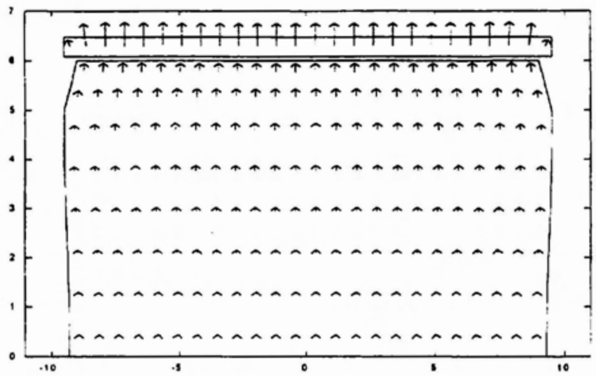

FIGURE 5 HEAT FLUX PROFILE IN PELLET AND SHEATH (CASE 2)

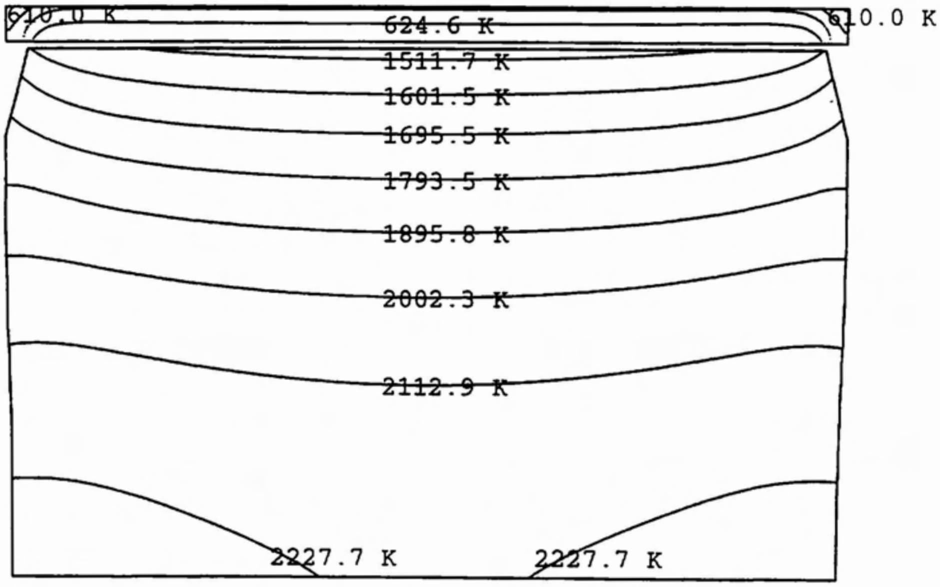

FIGURE 6 ISOTHERMS IN PLANE θ = 0° (CASE 2)

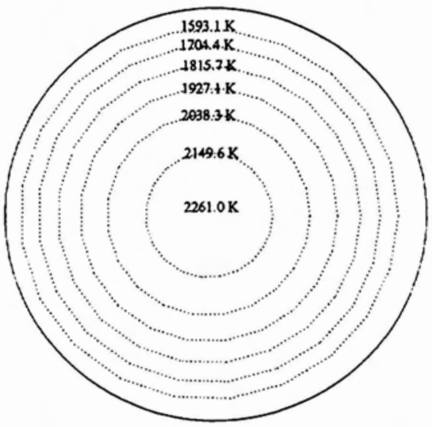

FIGURE 7 ISOTHERMS IN THE PELLET MIDPLANE (CASE 2)